

AN ALGORITHM FOR AUTOMATIC GENERATION CONTROL OF IRAQI POWER SYSTEM USING FUZZY LOGIC TECHNIQUE

Afaneen Anwer Alkhazraji ¹, Ihab salim ²

¹ Assistant Professor

Department of Electrical Engineer, University of Technology-Baghdad, Iraq

E-mail: afaneenalkhazragy@yahoo.com

(Received: 29/1/2015; Accepted: 7/6/2015)

ABSTRACT: This work proposes an algorithm based on Fuzzy Logic technique for the AGC of a power system controller to enhance the performance of the conventional controller during normal and abnormal condition (variation of load). The dynamic responses of Iraqi super grid network (400 kV) under normal and 10% step load increase (as a severe condition) to investigate using the fuzzy logic -PID controller and a conventional PID controller in MATLAB/SIMULINK environment. The obtained results show the proposal intelligent controller and have improved the dynamic response of the Iraqi grid, and at the same time, It is faster than the conventional PID controller in terms of reducing settling time, overshoot and oscillations.

Keywords: Automatic generation control, Fuzzy logic controller, Iraqi super grid network, MATLAB/SIMULINK environment.

1- INTRODUCTION

A modern power system network has consisted of a number of utilities interconnected together and power has exchanged between utilities over tie-line by which they have interconnected. An electrical power system must be maintained at a desired operating level characterized by nominal frequency, voltage profile and load flow conditions. It has kept in its nominal state by close control of real and reactive powers generated by the controllable sources in the system. Due to the inherent characteristics of changing loads, the operating point of power system has changed very much during a daily cycle. The generation changes have made to match the load perturbation at the nominal conditions, if the normal state has to be maintained ^[1].

The problem of controlling the real power output of electric generators has termed as Automatic Generation Control (AGC). AGC has summarily defined as: The regulation of the power output of electric generators within a prescribed area due to the changes in system frequency and/or tie line loading, so as to maintain the schedule system frequency and/or the established interchange with other areas within predetermined limits ^[2]. In practice different conventional control strategies have being used for AGC. Yet, the limitations of conventional PI and PID controllers have: slow and lack of efficiency and poor handling of system nonlinearities. Artificial Intelligence techniques have liked Fuzzy Logic, Artificial Neural networks, Genetic Algorithms (GA) and Particle Swarm Optimization (PSO) can be applied for automatic generation control, which can overcome the limitations of conventional controls as PID control, but Fuzzy has the most suitable AI techniques related to control applications ^[3]. There have being continued efforts for designing LFC controllers by using various adaptive neural networks and robust methods. Shankar^[4] has presented an optimal

fuzzy controller design for load frequency control (LFC) of two area power system using Adaptive Particle Swarm Optimization (APSO). The controller is designed according to Fuzzy Logic rules then, It has optimized with PSO so as to obtain optimal adjustment of the membership functions only. Simulation results have demonstrated that in comparison with the FLC, the designed FLC-APSO speed controller gives better dynamic performance of the LFC, as well as without any overshoot. Sinha^[5] has tried out the optimized controllers, namely PSO tuned FLC and GA tuned FLC controllers, for AGC of a three area thermal-thermal-hydro system. Analyses of these responses have clearly revealed that GA tuned FLC and PSO tuned FLC provide better dynamic responses compared to the FLC. Presence of FLC in all the areas guarantees zero steady state error; but GA tuned and PSO tuned FLCs provide less peak overshoot and the settling time has also less. Parveen^[6] has described the design, implementation, and the operation performance of Fuzzy controller as part of the combined loop of AGC& AVR for single area thermal power system. The Fuzzy controller has implemented in the control of ACE calculation in the case of AGC and excitation in case of AVR. Falehi^[7] attained a novel Fuzzy Logic Automatic Generation Controller (FLAGC) to provide appropriate damping low frequency power oscillations. It has compared with Proportional Integral Derivative (PID) controller considering 2% step load perturbation in thermal area of the studied power system. The obtained results have of non-linear time-domain simulation revealed the high dynamical performance of proposed FLAGC controller. Afshan^[8] has presented different methods regarding the tuning of conventional PID and fuzzy logic controller. Simulation has carried out using MATLAB version 2010a to get the output response of the system. The amount of overshoot for the output response has successfully decreased by using the fuzzy logic controller; the improved performance has to the cost of increase rise-time and settling-time. The performances of different processes by using different defuzzification methods have also presented in this paper. From the obtained results, It was observed that except the value of the percentage overshoot Mean of Maximum defuzzification method which has given better results as compared to other defuzzification techniques.

This work has proposed an approach based on a Fuzzy Logic - PID controller to improve the dynamic performances of the Iraqi power system under a variety of operating condition

2. PROBLEM FORMULATION^[9-11]

An interconnected power system has divided into control areas connected by a tie line. In each control area, all generators have supposed to constitute a coherent group. If the loads of an area have changed by ΔP_{Di} , the generation would be changed by ΔP_{gi} due to the action of the turbine controllers. The net power surplus in the area following a disturbance has equal to $(\Delta P_{gi} - \Delta P_{Di})$, compensated by the change in the kinetic energy of the area. The value $\frac{d}{dt} (W_{Kin,i})$ which has known as the kinetic energy has proportional to the square of the speed, therefore area kinetic energy can be expressed as:

$$W_{Kin,i} = W_{Kin,i}^* \left(\frac{f}{f^*} \right)^2 \quad (1)$$

Therefore

$$\begin{aligned} \frac{d}{dt} W_{Kin,i} &= \frac{d}{dt} \left(W_{Kin,i}^* \left(\frac{f}{f^*} \right)^2 \right) \\ &= \frac{d}{dt} \left(W_{Kin,i}^* \left(1 + \frac{2\Delta f_i}{f^*} \right) \right) \\ &= 2 W_{Kin,i}^* f^* \frac{d}{dt} (\Delta f_i) \end{aligned} \quad (2)$$

The change in the load, due to the variation of the frequency has equal to:

$$D_i = \frac{\partial PL_i}{\partial F} \text{ p.u.MW / Hz}$$

The variation of the export of power via the tie-line (ΔP_{ti}) which has called “power equilibrium” expressed by:

$$\Delta P_{gi} - \Delta P_{Di} = 2 \frac{W_{Kin,i}^*}{f^*} \frac{d}{dt} (\Delta f_i) + D_i \Delta f_i + \Delta P_{tie,i} \quad (3)$$

Dividing equation (3) by (P_{ri}), total rated area (i) power has given as:

$$\Delta P_{gi} - \Delta P_{Di} = \frac{2H_i}{f^*} \frac{d}{dt} (\Delta f_i) + D_i \Delta f_i + \Delta P_{tie,i} \quad (4)$$

Where : $H_i = W_{Kin,i}^* / P_{ri}$

If several generating sets are operating in parallel, It have one end of an interconnector. And the transfer reactance between these sets can be neglected relative to the reactance of the interconnector. Eq. (4) can be written as

$$d/dt (\Delta f_i) = (\Delta P_{gi} - \Delta P_{Di} - \Delta P_{tie,i} - \frac{1}{k_{pi}} \Delta f_i) \frac{k_{pi}}{T_{pi}} \quad (5)$$

Where : $T_{pi} = \frac{2H_i}{(f^* D_i) \text{ sec}}$

And $k_{pi} = \frac{1}{D_i} \frac{\text{Hz}}{\text{pu}}$

Taking the Laplace transformation of Eq. (5) results in:

$$\Delta f_i = \left(\frac{k_{pi}}{1 + sT_{pi}} \right) (\Delta P_{gi}(s) - \Delta P_{Di}(s) - \Delta P_{tie,i}(s)) \quad (6)$$

The system output depends on area control error (ACE) which can be defined by:

$$ACE_i = \Delta P_{ij} + \beta_i * \Delta f \quad (7)$$

$$\beta_i = D_i + \frac{1}{R_i} \frac{\text{p.u.MW}}{\text{Hz}} \quad (8)$$

Where i : control area for which ACE is being measure.

ΔP_{ij} : power interchange in areas i and j, (P_{Tij})

B_i : control area frequency bias coefficient

Δf :deviation in frequency

The task of load frequency controller has to generate a control signal U_i that maintains system frequency and tie-line interchange power at predetermined values the control input U_i is constructed as follows:

$$U_i = K_i \int_0^T (ACE_i) dt = - K_i \int_0^T (\Delta P_{Tie,i} + B_i \Delta F_i) dt \quad (9)$$

Taking the derivative of equation (9) yields

$$U_i = K_i (ACE_i) = - K_i (\Delta P_{Tie,i} + B_i \Delta F_i) \quad (10)$$

3. FUZZY LOGIC CONTROLLER [12-15]

Fuzzy logic system control has considered as a branch of artificial intelligent expert systems that have distinguished by characteristics making them powerful in control application. Its rules have constructed by expert experience or knowledge database.

The fuzzy logic controller has comprised of three main components:

- Fuzzifier.
- Rule base and inference engine (control unit).
- Defuzzifier.

3.1 FUZZYFIER

The first step in designing a fuzzy controller has to decide which state variables represent the system dynamic performance have taken as the input signal to the controller. Fuzzy logic has used linguistic variables instead of numerical variables. The process of converting a numerical variable (real number or crisp variables) into a linguistic variable (fuzzy number) has called Fuzzification. System variables, which have usually used as the fuzzy controller inputs includes states error, state error derivative, state error integral or etc. In power system, based on previous experience, Area Control Error (ACE) and its derivative (d (ACE)/dt) have chosen to be the input signals of fuzzy AGC. The membership function is a graphical representation of the magnitude of participation of each input. There are different memberships functions associated with each input and output response. In this study, the triangular membership functions for input and output variables have used. For the AGC study, seven linguistic variables for each of the input and output variables have used to describe them. As shown in table (1).

3.2 RULE BASE AND INFERENCE ENGINE

The rules have in the following format. If error has A_i , and change in error has B_i then output C_i . Here the “if” part of a rule has called the *rule-antecedent* and for a description of a process state in terms of a logical combination of atomic fuzzy propositions. The “then” part of the rule has called the rule consequent and has a description of the control output in terms of a logical combination of fuzzy propositions.

3.3 DEFUZZIFICATION

The reverse of Fuzzification has called *Defuzzification*. The use of Fuzzy Logic Controller (FLC) produces have required output in a linguistic variable (fuzzy number). According to real world requirements, the linguistic variables have to be transformed to crisp output. There have various techniques for defuzzification, but the Centre of gravity method Mamdani type has the best well-known defuzzification method to use in this field. It has obtained the center of area occupied by the fuzzy set. It has given by the expression:

$$X = \frac{\int M(x) \cdot x \, dx}{\int M(x) \, dx} \quad (11)$$

4. STRUCTURE OF THE PROPOSED CONTROLLER

The controller has consisted of Fuzzy PD control with parallel integral action (fuzzy PD+I) The structure of this approach can be achieved by placing a conventional integral controller in parallel with the fuzzy PD controller as it has shown in Figure (1) .The control action has obtained with the output from the fuzzy PD controller and the output from the conventional integral controller.

$$u(n) = u_{pd}(n) + K_i \sum_{q=1}^n e(q) \quad (12)$$

Where: K_i has some integral gain that has to be determined

The advantage of this approach has the integral action can remove the system steady state error. To achieve a first response, the integral action can be large, i.e. the integral gain K_i can be large. As the phase-lag of the first order system has small, fuzzy PD+I control can achieve good result with a large integral action. This type of controller is the one adopted in this work. The calculation of the control action in the fuzzy Logic algorithm has consisted of following four steps:

1. Calculate area control error (ACE) and change of frequency (Δf).
2. Convert the error and change of frequency into fuzzy variables i.e. linguistic variables such as Positive Big (PB), Positive Medium (PM) etc., as given below.
3. Evaluate the decision rules, rule base by using the compositional rule of inference.

4. Calculate the deterministic input required to regulate the process. The control rules are formulated in linguistic terms by using fuzzy sets to describe the magnitude of error, the frequency deviation and the magnitude of the appropriate control action.

Figure (2) shows the flow- chart of the controller.

5. THE PAREMETRES OF THE PROPOSED CONTROLLER

The Fuzzy Logic controller has run with inputs and output of a normalized universe of [-1, 1].

The two inputs to the fuzzy PID-controller have (e and Δe) mimicking the error frequency and changing in the error frequency respectively.

The parameters of the proposed controller were selected as follow:

- Rule base: The Mamdani-type rule-base has selected to ensure stability and quality with seven membership functions.
- Type of membership function: The member ship function for ($e, \Delta e, \&u$) is a triangular shape.
- Defuzzification method: the selected method has the centroid method.

6. AGC PERFORMANCE OF IRAQI SUPER GRID NETWORK

The transmission level in the Iraqi electrical network has consisted of the 400 kV network, and the 132 kV network connected to it. The aim of this work has limited to the 400 kV network with all its buses and transmission lines. The network under consideration has consisted of 24 buses (11 generation buses and 13 load buses) and 40 transmission lines; with total length of 3979 Km. The total installed generation capacity is 5840 MW, the line data and bus data have given in the appendix these values have calculated by a load flow program written in MATLAB language (version 7.10), using Newton Raphson method. Figure (3) shows a configuration of this network.

In this work the eleven generation buses have considered as eleven-control areas. These areas have represented according to their types (thermal, hydro and gas). Conventional integral controller and FL-PID controller design has accomplished by trial-and-error methods using computer simulations. The Matlab Simulink block diagram with the proposed FL-PID controller is shown in Figure (4). The system parameters data have given in Appendix A.

Depending on the type of the area: The membership functions for ($e, \Delta e, \&u$) and the seven linguistic variables used for each e and Δe as inputs and the 49 rules of u (output) have shown in appendix B. To study and analyze the effect of a load change on the frequency, tie-line power and generator output, a (10) % step load change has assumed to take place at: Baiji power station. The system responses to a (10) % step load change in Baiji power stations have shown in the appendix C with conventional integral controller (red) and with fuzzy PID-controller (blue).

7. DISCUSSION

The aim of this work has to improve the AGC performance of the power system by adopting new algorithm for FL-PID controller. The controller has been tested on the Iraqi super grid. This system has contained eleven areas, hydro areas (1,5), thermal areas (2,8,9,11) and gas areas (3,4,6,7,10). Studying the simulation results for the tie-line power, generator power and frequency of each area shown in the appendix C (Figures 1-38), a comparison between the results of the conventional and the proposed FL-PID controller has presented in table (4 a and b).

The results have obtained in table (4) shows,

- The reduction of the settling time of the frequency has 70 - 75% for area one
- Three, five, six, seven, and eight. 80% for area four. 63 - 67 % for area two, nine, ten, and eleven.

The decrement of the frequency undershoots have 31 - 35% for area one, two, nine, and ten, 41 % for area three, 21-23 % for area four, five, seven, and eleven, 19% for area six, and 17% for area eight.

- The reduction of the settling time of the generated power has 25% for area one (ΔP_{g1}), 75% for area two (ΔP_{g2}), 67% for area three (ΔP_{g3}), 67% for area four (ΔP_{g4}), 17% for area five (ΔP_{g5}), 65% for area six (ΔP_{g6}), 64% for area seven (ΔP_{g7}), 82% for area eight (ΔP_{g8}), 81% for area nine (ΔP_{g9}), 68% for area ten (ΔP_{g10}), 67% for area eleven (ΔP_{g11}),

While the overshoot reduction has 38% for area one, without for area two (step output), 46% for area three, 40% for area four, 64% for area five, 29% for area six, 25% for area seven increased the overshoot by 14% for area eight and 9% for area nine, the reduction of the overshoot by 33% for area ten. The overshoot for the eleventh area is the same.

- The reduction of the settling time of power for the tie-line between area one and two ($\Delta P_{tie_{1,2}}$) has 40%, 70-79 % for the tie-line between area two and three ($\Delta P_{tie_{2,3}}$), area two and five ($\Delta P_{tie_{2,5}}$), area two and eight ($\Delta P_{tie_{2,8}}$), area three and four ($\Delta P_{tie_{3,4}}$), area five and seven ($\Delta P_{tie_{5,7}}$), area five and eight ($\Delta P_{tie_{5,8}}$), and area six and seven ($\Delta P_{tie_{6,7}}$), area eight and nine ($\Delta P_{tie_{8,9}}$), area nine and ten ($\Delta P_{tie_{9,10}}$). 38% for the tie-line between area four and six. ($\Delta P_{tie_{4,6}}$) 85% for the tie-line between area six and eight ($\Delta P_{tie_{6,8}}$), 58% for the tie-line between area six and nine ($\Delta P_{tie_{6,9}}$), 60- 62% for the tie-line between area seven and eight ($\Delta P_{tie_{7,8}}$), area nine and eleven ($\Delta P_{tie_{9,11}}$), and area ten and eleven ($\Delta P_{tie_{10,11}}$).

while the undershoot has decreased by 7% for $\Delta P_{tie_{1,2}}$, 18% for $\Delta P_{tie_{2,3}}$, 15% for $\Delta P_{tie_{2,5}}$, 12% for $\Delta P_{tie_{2,8}}$, 9% for $\Delta P_{tie_{3,4}}$, the undershoot increases by 17% for $\Delta P_{tie_{4,6}}$, while decreases by 15% for $\Delta P_{tie_{5,7}}$, 9% for $\Delta P_{tie_{5,8}}$, 16% for $\Delta P_{tie_{6,7}}$, 19% for $\Delta P_{tie_{6,8}}$, 6% for $\Delta P_{tie_{6,9}}$, 10% for $\Delta P_{tie_{7,8}}$, 17% for $\Delta P_{tie_{8,9}}$, 8% for $\Delta P_{tie_{9,10}}$, the undershoot increases by 6% for $\Delta P_{tie_{9,11}}$ and 8% for $\Delta P_{tie_{10,11}}$.

From the results obtained, It has very clear that using the proposed fuzzy-PID controller improved the dynamic response of the network by reducing the settling time and the peak overshoot and undershoots.

8. CONCLUSION

Automatic Generation Control (AGC) plays a very important role in power system; its main role is to maintain the system frequency and tie line flow at their scheduled values during normal period in an interconnected system. This work presents the performance of AGC for Iraqi super grid (400 kV) using FL-PID controller. The conventional and the proposed FL-PID controller has tested. The changes in the generation and in overall frequency of each area were examined using MATLAB/ SIMULINK under changing loads (10% step load change). Area control error has measured and the results of the conventional method and the fuzzy logic have compared. The results have shown that the proposed controller provided a satisfactory stability between frequency overshoot and dynamic oscillations with zero steady state error. It has improved the dynamic responses and reduced the settling time, overshoot and oscillations.

REFERENCES

1. Wood A. J., Woolenber B. F. (1984), "Power Generation Operation and Control", John Wiley and Sons.
2. Gopal M., (1993), "Modern control system theory", Wiley Eastern Ltd., 2nd Edition.
3. Elgerd O. I., (2001), "Electric energy Systems Theory – An Introduction", McGraw Hill Co..

4. Naik R.S., Sekhar K. CH., Vaisakh K., (2009), "ADAPTIVE PSO BASED OPTIMAL FUZZY CONTROLLER DESIGN FOR AGC EQUIPPED WITH SMES AND SPSS", Journal of Theoretical and Applied Information Technology, vol. 7, No.1, pp 008-017.
5. Sinha S. K., Patel R. N., Prasad R., (2010), " Application of GA and PSO Tuned Fuzzy Controller for AGC of Three Area Thermal- Thermal-Hydro Power System", International Journal of Computer Theory and Engineering, Vol. 2, No. 2, 1793-8201.
6. Dabur P., Kumar N., Avtar R., (2012), "Matlab Design and Simulation of AGC and AVR for Single Area Power System with Fuzzy Logic Contrilar", International Journal of Soft Computing and Engineering, volume 1, Issue 6.
7. Falehi A. D., Atabakhsh M., (2013), " Robust AGC based on Fuzzy Logic Controller: Design, Comparison and Ratification", Research Journal of Applied Sciences, Engineering and Technology, 6(10): 1813-1817.
8. Ilyas A., Jahan S., Ayyub M., (2013), "Tuning Of Conventional Pid And Fuzzy Logic Controller Using Different Defuzzification Techniques", INTERNATIONAL JOURNAL OF SCIENTIFIC & TECHNOLOGY RESEARCH, VOLUME 2, ISSUE 1.
9. Hassan B., (2009), "Robust Power System Frequency Control", Springer Science & Business Media.
10. Saadat H., (1999), "Power System Analysis", McGraw-Hill Inc.,.
11. AL-Hayali W. S., (2003), "Small Perturbation Stability Improvement of Electric Power System Using Neural Network", Department of Education Technology Engineering, University of Technology, Ph.D. Thesis.
12. AL- Sujada J. S., (2007), "Enhancement of Transient Stability for Iraqi Power System by using Fuzzy-Genetic Controller", Department of Electrical and Electronic Engineering, University of Technology, Ph.D. Thesis.
13. Lee K. H., (2005), "Advances in Soft Computing", Springer-Verlag Berlin Heidelberg.
14. Jantzen J., (1998), "Design of Fuzzy Controllers", Tech. Report No.98 –E 864 Technical University of Denmark, Department of Automation, <http://www.iau.dtu.dk/~jj/pubs/design.pdf>, Aug..
15. Zhang R., Phillis Y. A., Kouikoglou V. S., (2005), "Fuzzy Control of Queuing Systems", Springer-Verlag London Limited.

Table -1- Fuzzy Linguistic Variables

LN	Large Negative
MN	Medium Negative
SN	Small Negative
Z	Zero
SP	Small Positive
MP	Medium Positive
LP	Large Positive

Table (4-a): Comparisons for Iraqi super with conventional and FL-PID controller

	State Variable	Settling time, sec		Maximum Overshoot/ Under shoot (Pu)	
		System with integral controller	System with fuzzy-PID controller	System with integral controller	System with fuzzy-PID controller
Area.1	$\Delta\omega_1$	500	125	2.6×10^{-3}	1.7×10^{-3}
	$\Delta P g_1$	400	300	0.024	0.015
Area.2	$\Delta\omega_2$	450	150	2.62×10^{-3}	1.8×10^{-3}
	$\Delta P g_2$	450	125	---	---
Area.3	$\Delta\omega_3$	500	150	2.52×10^{-3}	1.5×10^{-3}
	$\Delta P g_3$	425	140	0.065	0.035
Area.4	$\Delta\omega_4$	490	100	2.25×10^{-3}	1.78×10^{-3}
	$\Delta P g_4$	455	152	0.0565	0.034
Area.5	$\Delta\omega_5$	500	145	2.25×10^{-3}	1.75×10^{-3}
	$\Delta P g_5$	360	300	0.025	0.009
Area.6	$\Delta\omega_6$	490	140	2.6×10^{-3}	2.1×10^{-3}
	$\Delta P g_6$	425	148	0.063	0.045
Area.7	$\Delta\omega_7$	500	138	2.46×10^{-3}	1.9×10^{-3}
	$\Delta P g_7$	420	151	0.06	0.045
Area.8	$\Delta\omega_8$	520	130	2.3×10^{-3}	1.9×10^{-3}
	$\Delta P g_8$	450	80	0.043	0.05
Area.9	$\Delta\omega_9$	480	150	2.65×10^{-3}	1.8×10^{-3}
	$\Delta P g_9$	475	90	0.05	0.055
Area.10	$\Delta\omega_{10}$	450	138	2.6×10^{-3}	1.7×10^{-3}
	$\Delta P g_{10}$	460	148	0.063	0.042
Area.11	$\Delta\omega_{11}$	400	149	2.85×10^{-3}	2.2×10^{-3}
	$\Delta P g_{11}$	445	148	0.06	0.06

Table (4-b): Comparisons for Iraqi super with conventional and FL-PID controller

	State Variable	Settling time, sec		Maximum Overshoot/ Under shoot (Pu)	
		System with integral controller	System with fuzzy-PID controller	System with integral controller	System with fuzzy-PID controller
Tie-Line 1,2	$\Delta P_{tie_{1,2}}$	350	210	0.15	0.14
Tie-Line 2,3	$\Delta P_{tie_{2,3}}$	490	140	0.098	0.08
Tie-Line 2,5	$\Delta P_{tie_{2,5}}$	450	130	0.13	0.11
Tie-Line 2,8	$\Delta P_{tie_{2,8}}$	440	130	0.26	0.23
Tie-Line 3,4	$\Delta P_{tie_{3,4}}$	425	125	0.064	0.058
Tie-Line 4,6	$\Delta P_{tie_{4,6}}$	160	100	0.025	0.03
Tie-Line 5,7	$\Delta P_{tie_{5,7}}$	470	100	0.08	0.068
Tie-Line 5,8	$\Delta P_{tie_{5,8}}$	500	140	0.044	0.04
Tie-Line 6,7	$\Delta P_{tie_{6,7}}$	400	100	0.043	0.036
Tie-Line 6,8	$\Delta P_{tie_{6,8}}$	390	60	0.093	0.075
Tie-Line 6,9	$\Delta P_{tie_{6,9}}$	350	150	0.034	0.032
Tie-Line 7,8	$\Delta P_{tie_{7,8}}$	375	145	0.04	0.036
Tie-Line 8,9	$\Delta P_{tie_{8,9}}$	500	150	0.18	0.15
Tie-Line 9,10	$\Delta P_{tie_{9,10}}$	500	150	0.081	0.075
Tie-Line 9,11	$\Delta P_{tie_{9,11}}$	390	150	0.033	0.035
Tie-Line 10,11	$\Delta P_{tie_{10,11}}$	350	140	0.046	0.05

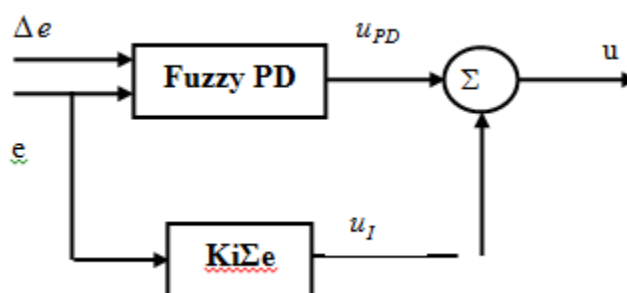


Figure (1) Fuzzy PD control with deterministic integral control.

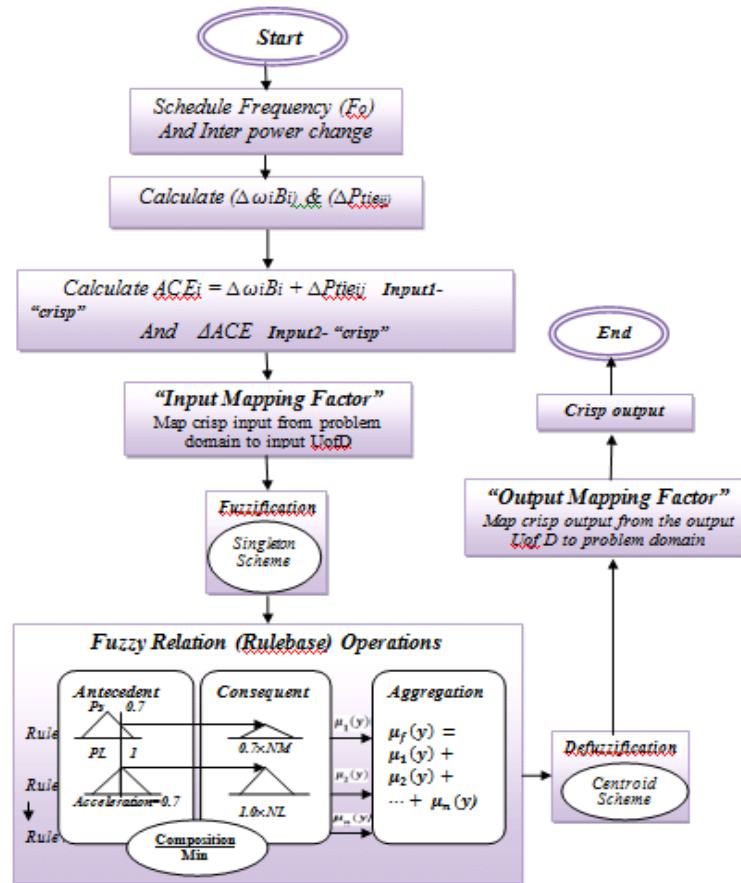


Figure (2) the flow- chart of the FL-PID controller

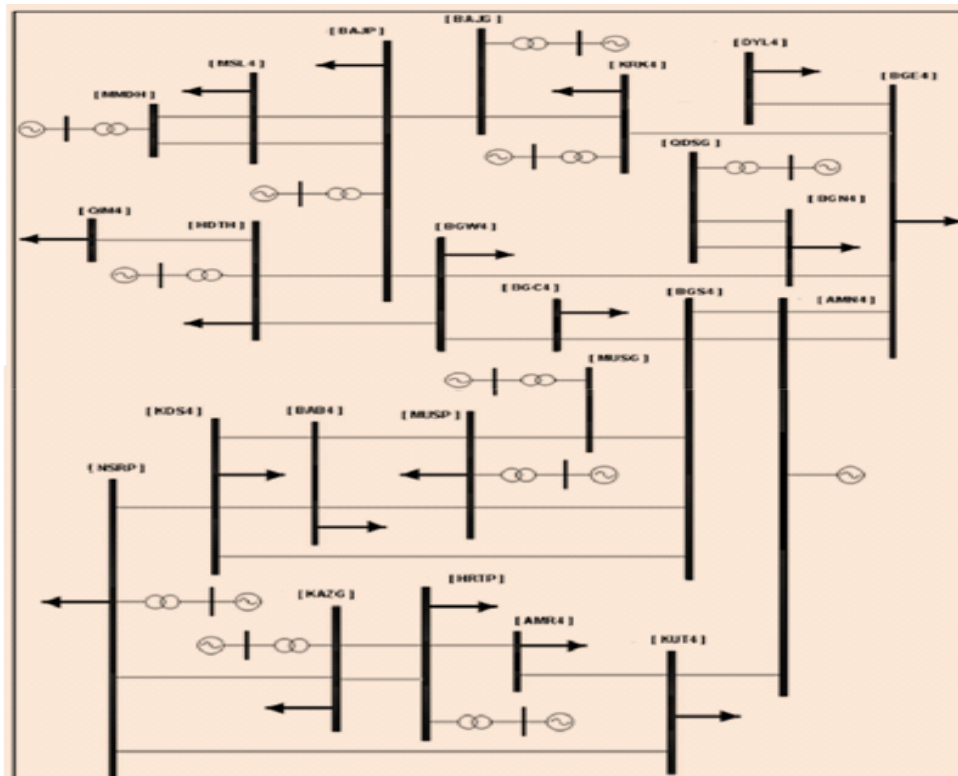


Figure (3) Iraqi super grid network configuration

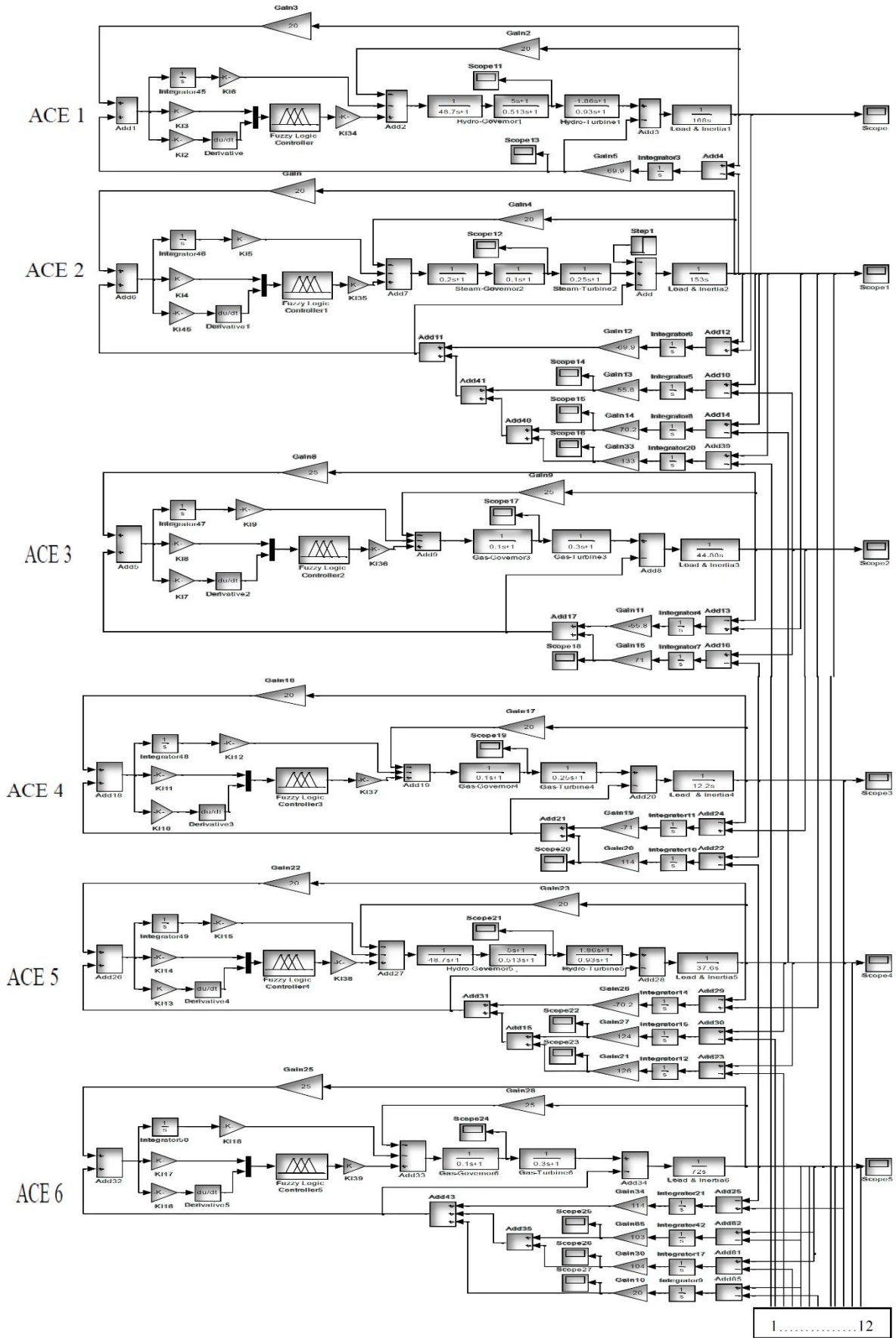


Figure (4) Block diagram of Iraqi super grid with FL- PID controller (A)

Appendices

Appendix (A): Data of the Iraqi Power Grid (400 kV)

Table (A-1): Type of plants and their speed governor

Name of Plants	Types of Plants	Turbine and Speed Governor Types
MMDH	Hydro	Francis
BAJP	Thermal	Non-reheat type 10
BAJG	Gas	Gas
KRK4	Gas	Gas
HDTH	Hydro	Caplin, type 12
MUSP	Thermal	Reheat
KAZG	Gas	Gas
H RTP	Thermal	Non-reheat type 10
NSRP	Thermal	Non-reheat type 10
MUSG	Gas	Gas
QDSG	Gas	Gas

Table (A-2): Parameters of the eleven area

Area No.	T_R Sec	T_{PV} Sec	T_2 Sec	T_3 Sec	T_W Sec	T_{CH} Sec	T_r Sec	K_r Sec	H Sec	R p.u	f Hz
1	5	48.7	0.513	---	1.86	---	---	---	84	0.05	50
2	---	0.2	0.0	0.1	---	0.25	---	---	76.5	0.05	50
3	---	0.1	---	---	---	0.3	---	---	22.4	0.04	50
4	---	0.1	---	---	---	0.25	---	---	6.1	0.04	50
5	5	48.7	0.513	---	1.86	---	---	---	18.8	0.05	50
6	---	0.1	---	---	---	0.3	---	---	36	0.04	50
7	---	0.1	---	---	---	0.32	---	---	18.5	0.04	50
8	---	0.1	0.0	0.0	---	0.25	6	0.5	93.5	0.05	50
9	---	0.1	0.0	0.12	---	7	---	---	93.5	0.05	50
10	---	0.1	---	---	---	0.3	---	---	14.4	0.04	50
11	---	0.1	0.0	0.12	---	7	---	---	38	0.05	50

Table (A-3): The voltage and angle of the generation bus bar.

Name of Area	Area - 1- MMH D	Area - 2- BAJP	Area - 3- BAJG	Area - 4- KRK4	Area - 5- HDTH	Area - 6- QDSG	Area - 7- MUSG	Area - 8- MUS P	Area - 9- NSRP	Area - 10- KAZG	Area - 11- H RTP
V(p.u)	1.020	1.025	1.025	1.022	1.030	1.008	1.040	1.040	1.020	1.010	1.015
Angle	5.656	2.976	3.016	1.011	-0.993	-2.274	-0.009	0.000	-9.496	-17.39	-17.40

Table (A-4): Transmission line parameters of the Iraqi network

<i>Line's name</i>	<i>R(p.u)</i>	<i>X(p.u)</i>	<i>B(p.u)</i>
<i>MMDH-MSL4</i>	<i>0.00144</i>	<i>0.01177</i>	<i>0.36439</i>
<i>MMDH-MSL4</i>	<i>0.00144</i>	<i>0.01177</i>	<i>0.36439</i>
<i>MSL4-BAJP</i>	<i>0.0042</i>	<i>0.03437</i>	<i>1.06426</i>
<i>MSL4-BAJP</i>	<i>0.0042</i>	<i>0.03437</i>	<i>1.06426</i>
<i>MSL4-KRK4</i>	<i>0.004984</i>	<i>0.04531</i>	<i>1.34251</i>
<i>BAJP-BAJG</i>	<i>0.00002</i>	<i>0.0002</i>	<i>0.00584</i>
<i>BAJP-BGW4</i>	<i>0.00483</i>	<i>0.04393</i>	<i>1.30165</i>
<i>BAJP-BGW4</i>	<i>0.00496</i>	<i>0.04511</i>	<i>1.33667</i>
<i>BAJP-HDTH</i>	<i>0.00345</i>	<i>0.03132</i>	<i>0.92808</i>
<i>BAJG-KRK4</i>	<i>0.0018</i>	<i>0.01635</i>	<i>0.48447</i>
<i>KRK4-BGE4</i>	<i>0.00496</i>	<i>0.04511</i>	<i>1.33667</i>
<i>BGW4-BGN4</i>	<i>0.00093</i>	<i>0.00847</i>	<i>0.25099</i>
<i>BGW4-BGC4</i>	<i>0.000672</i>	<i>0.006107</i>	<i>0.180947</i>
<i>BGW4-HDTH</i>	<i>0.00485</i>	<i>0.04405</i>	<i>1.30515</i>
<i>BGS4-AMN4</i>	<i>0.00082</i>	<i>0.00749</i>	<i>0.22181</i>
<i>BGS4-AMN4</i>	<i>0.00082</i>	<i>0.00749</i>	<i>0.22181</i>
<i>BGS4-BGC4</i>	<i>0.001105</i>	<i>0.010047</i>	<i>0.297687</i>
<i>BGS4-MUSP</i>	<i>0.00122</i>	<i>0.01015</i>	<i>0.31897</i>
<i>BGS4-MUSG</i>	<i>0.00122</i>	<i>0.01015</i>	<i>0.31897</i>
<i>BGS4-KDS4</i>	<i>0.00308</i>	<i>0.02795</i>	<i>0.82827</i>
<i>BGE4-BGN4</i>	<i>0.00029</i>	<i>0.00262</i>	<i>0.07763</i>
<i>BGE4-AMN4</i>	<i>0.00043</i>	<i>0.00394</i>	<i>0.11674</i>
<i>BGE4-DAL4</i>	<i>0.00087</i>	<i>0.00788</i>	<i>0.23348</i>
<i>BGN4-QDSG</i>	<i>0.00015</i>	<i>0.00138</i>	<i>0.04086</i>
<i>BGN4-QDSG</i>	<i>0.00015</i>	<i>0.00138</i>	<i>0.04086</i>
<i>AMN4-KUT4</i>	<i>0.003437</i>	<i>0.030382</i>	<i>0.910681</i>
<i>KUT4-NSRP</i>	<i>0.00432</i>	<i>0.03928</i>	<i>1.1639</i>
<i>KUT4-AMR4</i>	<i>0.00479</i>	<i>0.04354</i>	<i>1.28998</i>
<i>HDTH-QIM4</i>	<i>0.00292</i>	<i>0.02391</i>	<i>0.74035</i>
<i>MUSP-MUSG</i>	<i>0.000125</i>	<i>0.001043</i>	<i>0.032791</i>
<i>MUSP-BAB4</i>	<i>0.00081</i>	<i>0.00673</i>	<i>0.21165</i>
<i>MUSP-BAB4</i>	<i>0.00081</i>	<i>0.00673</i>	<i>0.21165</i>
<i>BAB4-KDS4</i>	<i>0.00233</i>	<i>0.01935</i>	<i>0.60812</i>
<i>BAB4-KDS4</i>	<i>0.00233</i>	<i>0.01935</i>	<i>0.60812</i>
<i>KDS4-NSRP</i>	<i>0.00383</i>	<i>0.03485</i>	<i>1.03256</i>
<i>NSRP-KAZG</i>	<i>0.00439</i>	<i>0.03993</i>	<i>1.18316</i>
<i>AMR4-HRTP</i>	<i>0.0029</i>	<i>0.0264</i>	<i>0.78216</i>
<i>HRTP-KAZG</i>	<i>0.00118</i>	<i>0.01076</i>	<i>0.3187</i>
<i>HRTP-KAZG</i>	<i>0.00118</i>	<i>0.01076</i>	<i>0.3187</i>
<i>KDS4- BGS4</i>	<i>0.003075</i>	<i>0.027954</i>	<i>0.82827</i>

Table (A-5) The load flow output for the Iraqi power system.

<i>B-B Name</i>	<i>V(p.u)</i>	<i>P_L(MW)</i>	<i>Q_L(MVAR)</i>	<i>P_g(MW)</i>	<i>Pr(MW)</i>
<i>MSUP</i>	1.0400	199.799	116.633	1107.1	1200.0
<i>MMDH</i>	1.0200	0	0	690.00	748.00
<i>BAJP</i>	1.0250	124.86	92.246	406.00	440.00
<i>BAJG</i>	1.0250	0	0	590.40	636.00
<i>KRK4</i>	1.0217	129.85	60.489	239.87	260.00
<i>MSUG</i>	1.0200	0	0	369.03	400.00
<i>HDTH</i>	1.0300	253.054	75.612	202.97	220.00
<i>QDSG</i>	1.0075	0	0	735.30	787.00
<i>KAZG</i>	1.0096	566.041	294.657	207.58	246.00
<i>H RTP</i>	1.0150	154.829	72.1171	332.13	400.00
<i>NSRP</i>	0.0197	422.866	198.321	774.97	840.00
<i>DAL4</i>	1.0000	83.200	21.172	0.0000	0.0000
<i>BGW4</i>	1.0000	576.031	302.448	0.0000	0.0000
<i>BGN4</i>	1.0000	412.877	139.126	0.0000	0.0000
<i>BGE4</i>	1.0000	849.062	294.654	0.0000	0.0000
<i>QIM4</i>	1.0000	109.878	39.318	0.0000	0.0000
<i>BGC4</i>	1.0000	49.949	181.468	0.0000	0.0000
<i>BGS4</i>	1.0000	0.0000	0.0000	0.0000	0.0000
<i>AMN4</i>	1.0000	126.564	56.001	180.00	0.0000
<i>MSL4</i>	1.0000	649.23	302.448	0.0000	0.0000
<i>BAB4</i>	1.0000	307.993	184.669	0.0000	0.0000
<i>KDS4</i>	1.0000	213.098	151.445	0.0000	0.0000
<i>KUT4</i>	1.0000	259.713	108.175	0.0000	0.0000
<i>AMR4</i>	1.0000	311.022	160.370	0.0000	0.0000

Table (A-6): The reactance between areas

<i>X_{ij}</i> (p.u)	<i>X_{1,2}</i>	<i>X_{2,3}</i>	<i>X_{2,5}</i>	<i>X_{2,8}</i>	<i>X_{3,4}</i>	<i>X_{4,6}</i>	<i>X_{5,7}</i>	<i>X_{5,8}</i>
	0.0153	0.0188	0.0150	0.0080	0.0146	0.0090	0.0086	0.0085
	<i>X_{6,7}</i>	<i>X_{6,8}</i>	<i>X_{6,9}</i>	<i>X_{7,8}</i>	<i>X_{8,9}</i>	<i>X_{9,10}</i>	<i>X_{9,11}</i>	<i>X_{10,11}</i>
0.0101	0.0100	0.0086	0.0155	0.0107	0.0199	0.0195	0.0347	

Table (A-7): The synchronising power between areas

<i>P_{ij}</i> (MW)	<i>Ps_{1,2}</i>	<i>Ps_{2,3}</i>	<i>Ps_{2,5}</i>	<i>Ps_{2,8}</i>	<i>Ps_{3,4}</i>	<i>Ps_{4,6}</i>	<i>Ps_{5,7}</i>	<i>Ps_{5,8}</i>
	69.9	55.8	70.2	133	71	114	124	126
	<i>Ps_{6,7}</i>	<i>Ps_{6,8}</i>	<i>Ps_{6,9}</i>	<i>Ps_{7,8}</i>	<i>Ps_{8,9}</i>	<i>Ps_{9,10}</i>	<i>Ps_{9,11}</i>	<i>Ps_{10,11}</i>
103	104	20	69	97	51	10	29.5	

Appendix B:

The triangle membership functions and the rule bases.

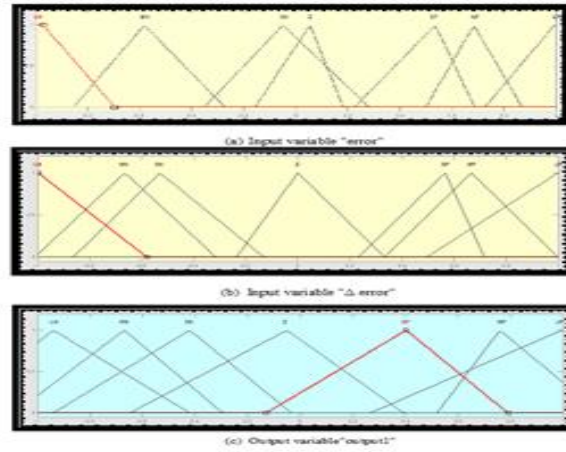


Figure (B1) Triangle membership functions for thermal area

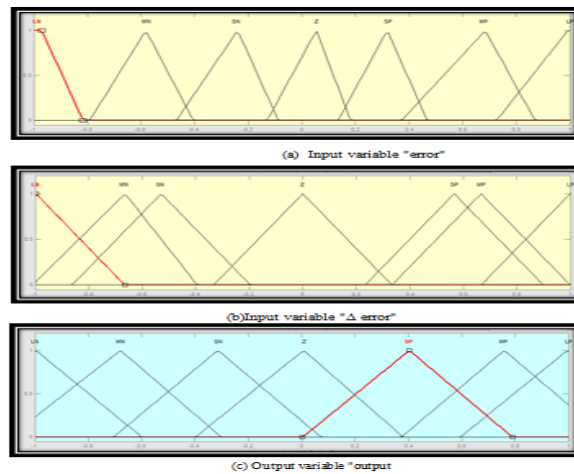


Figure (B2) Triangle membership functions for Gas area

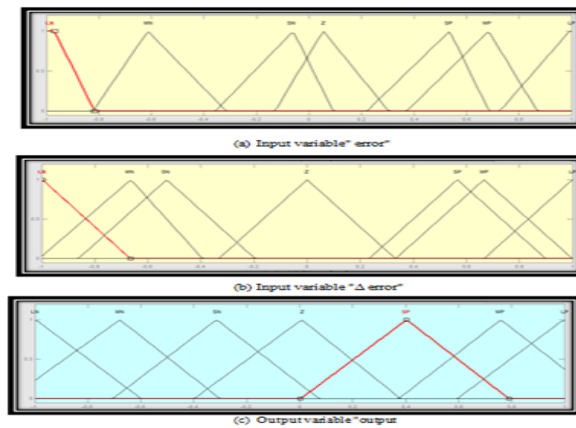


Figure (B3) Triangle membership functions for hydro area

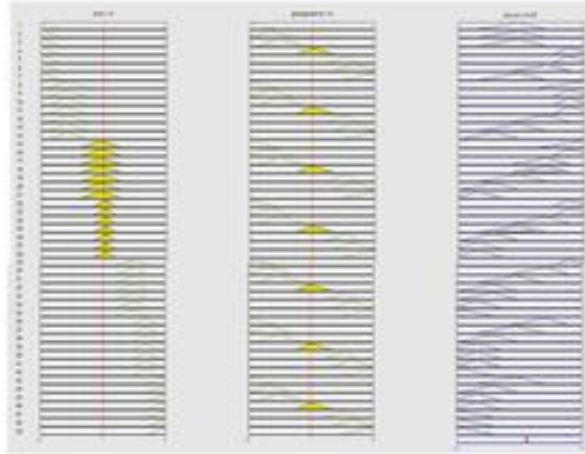


Figure (B4) The rule base for thermal area

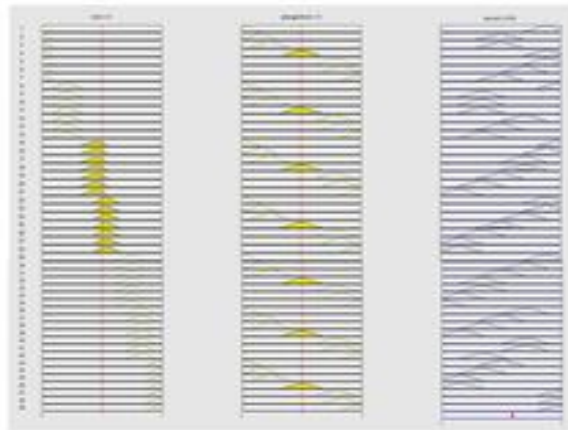


Figure (B5) The rule base for gas area

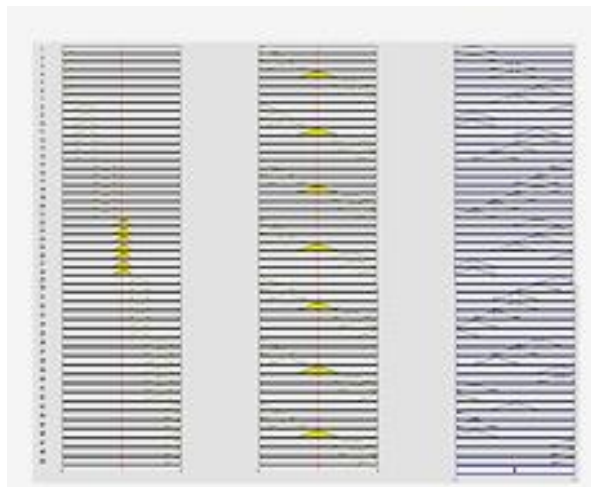


Figure (B6) The rule base for hydro area

Table (B.1) Rule Base of Fuzzy PID- Controller for Thermal area.

e Δe	LN	MN	SN	Z	SP	MP	LP
LN	Z	LP	LP	MP	MP	SP	Z
MN	Z	MP	MP	MP	SP	Z	SN
NS	Z	MP	SP	SP	Z	SN	MN
Z	MP	MP	SP	Z	SN	MN	MN
SP	MP	SP	Z	SN	SN	MN	LN
MP	SP	Z	SN	MN	MN	MN	LN
LP	Z	SN	MN	MN	LN	LN	LN

Table (B.2) Rule Base of Fuzzy PID- Controller for Hydro Area .

e Δe	LN	MN	SN	Z	SP	MP	LP
LN	MP	LP	LP	MP	MP	SP	Z
MN	Z	SN	MP	MP	SP	Z	SN
SN	Z	SN	SP	SP	Z	SN	MN
Z	MP	SN	SP	Z	SN	MN	MN
SP	MP	SP	Z	SN	SN	SP	LP
MP	SP	Z	SN	MN	MN	SP	LP
LP	Z	SN	MN	MN	LN	SN	LP

Table (B.3): Rule Base of Fuzzy PID- Controller for Gas Area.

e Δe	LN	MN	SN	Z	SP	MP	LP
LN	MN	LP	LP	SP	MP	SP	Z
MN	MN	MN	MP	MP	SP	Z	LN
SN	Z	MN	SP	SP	Z	SN	MN
Z	Z	SP	SP	Z	Z	MP	MN
SP	MP	SP	Z	LP	SN	MP	LP
MP	SP	Z	SN	MN	MN	MN	LP
LP	Z	SN	MN	MN	LN	LN	LP

Appendix C

The dynamic responses of the areas

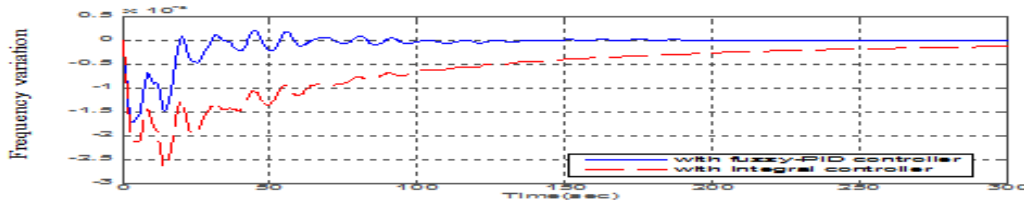


Figure (C1) Frequency response of area -1- ($\Delta\omega_1$)

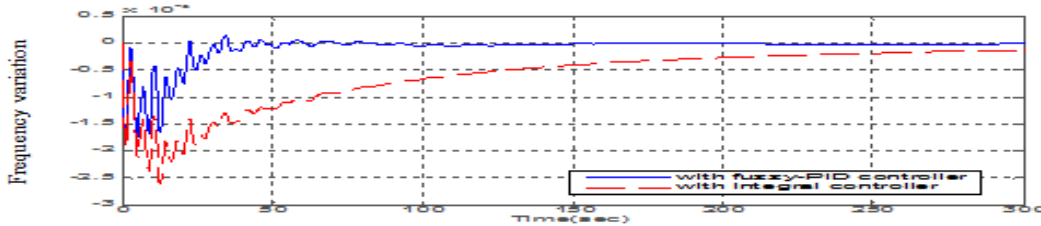


Figure (C2) Frequency response of area -2- ($\Delta\omega_2$)

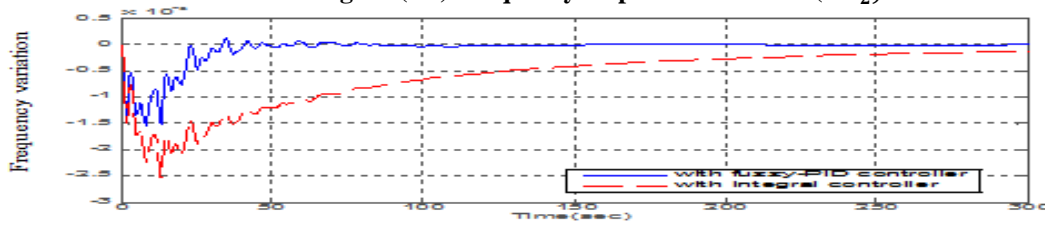


Figure (C3) Frequency response of area -3- ($\Delta\omega_3$)

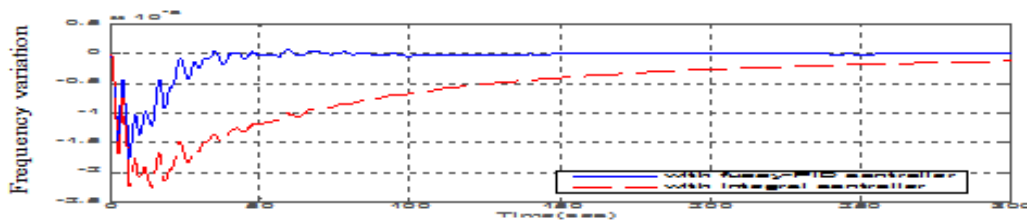


Figure (C4) Frequency response of area -4- ($\Delta\omega_4$)

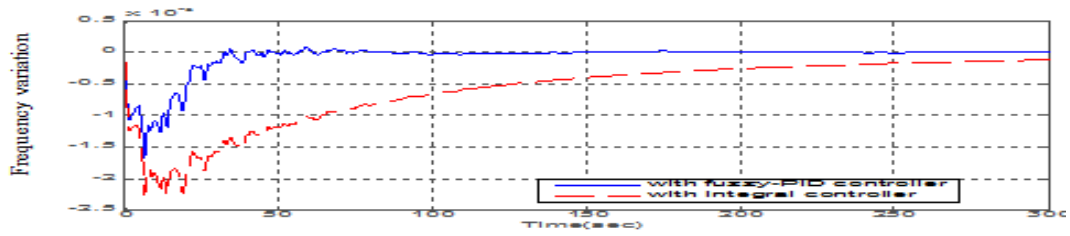


Figure (C 5) Frequency response of area -5- ($\Delta\omega_5$)

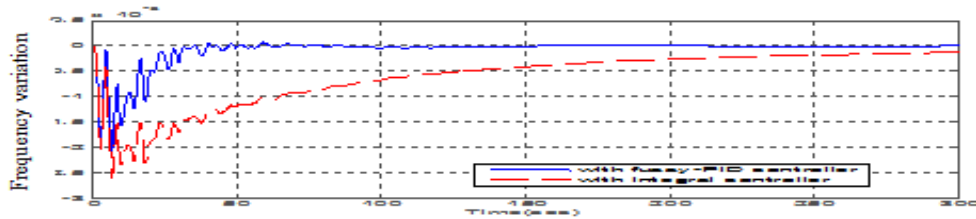


Figure (C 6) Frequency response of area -6- ($\Delta\omega_6$)

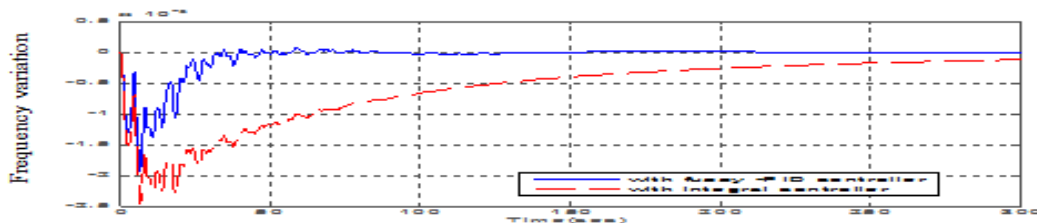


Figure (C 7) Frequency response of area -7- ($\Delta\omega_7$) –

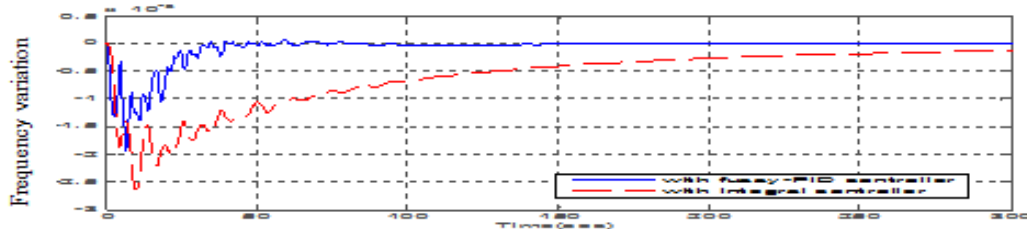


Figure (C 8) Frequency response of area -8- ($\Delta\omega_8$)

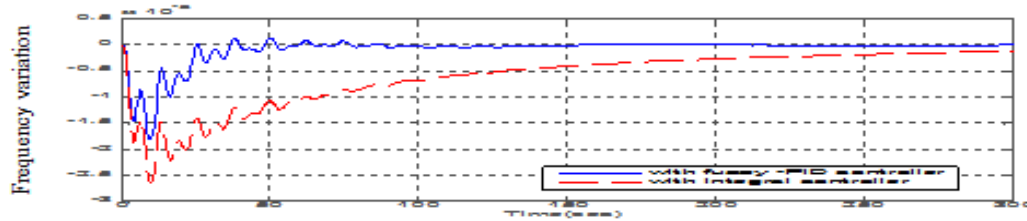


Figure (C 9) Frequency response of area -9- ($\Delta\omega_9$)

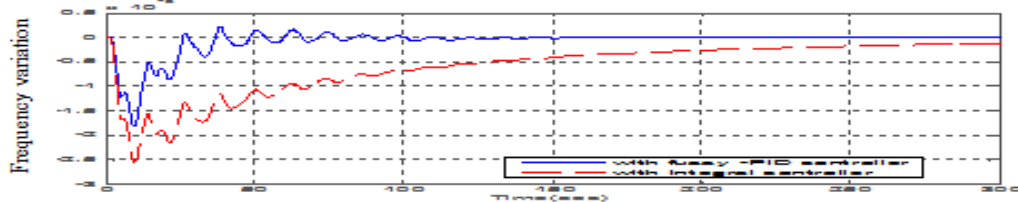


Figure (C 10) Frequency response of area -10- ($\Delta\omega_{10}$)

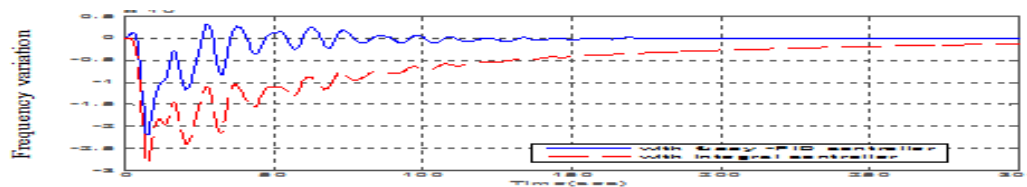


Figure (C 11) Frequency response of area -11- ($\Delta\omega_{11}$)

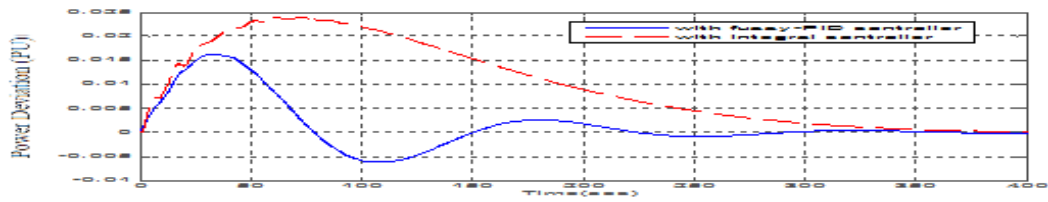


Figure (C 12) Generator output power of area -1-(ΔP_{g1})

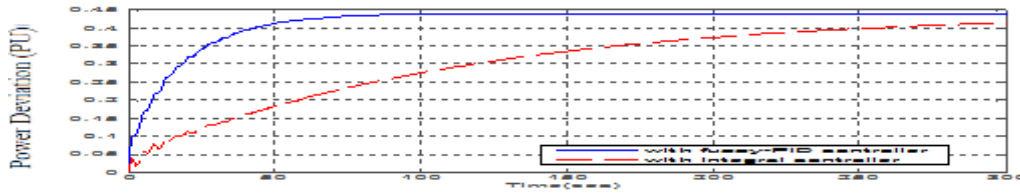


Figure (C 13) Generator output power of area -2-(ΔP_{g2})

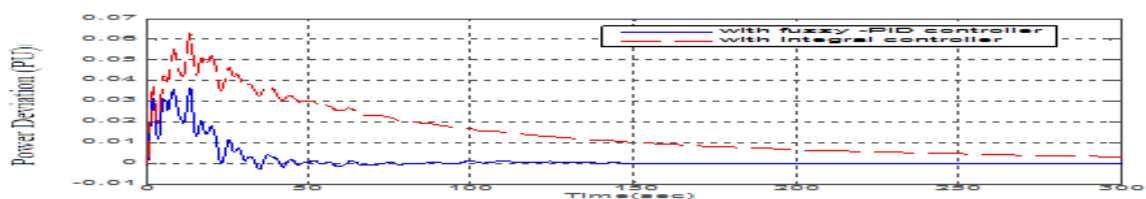


Figure (C 14) Generator output power of area -3-(ΔP_{g3})

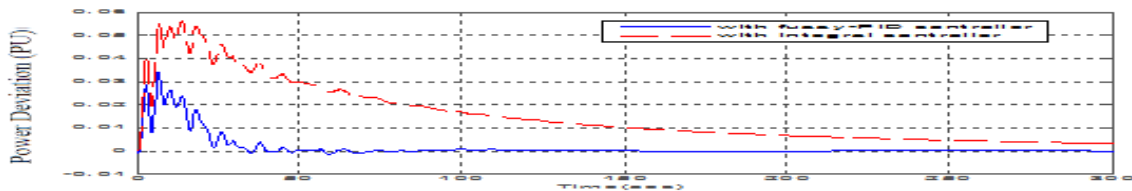


Figure (C 15) Generator output power of area -4-(ΔP_{g4})

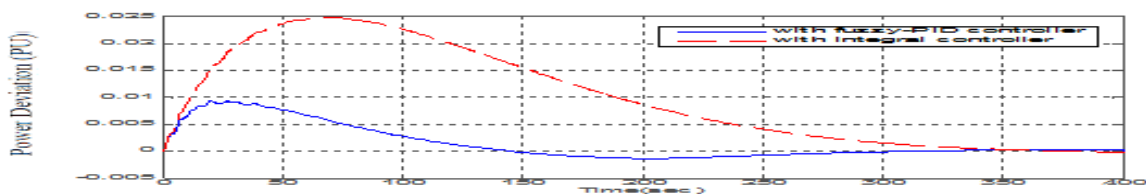


Figure (C 16) Generator output power of area -5-(ΔP_{g5})

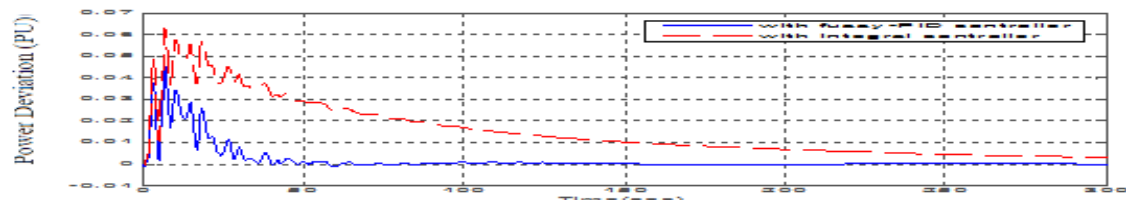


Figure (C 17) Generator output power of area -6-(Δg_6)

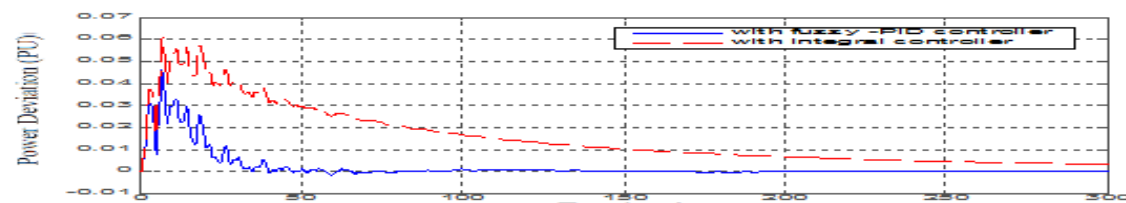


Figure (C 18) Generator output power of area -7-(ΔP_{g7})

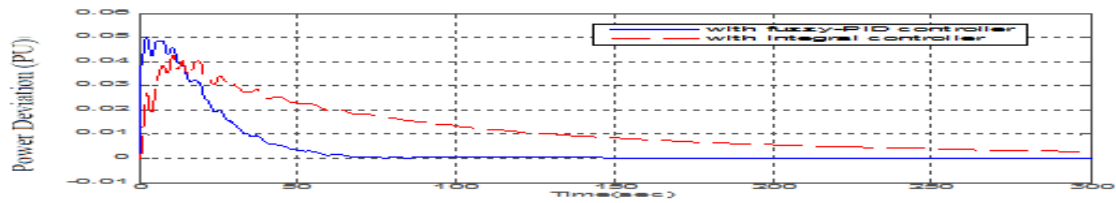


Figure (C 19) Generator output power of area -8-(ΔP_{g8})

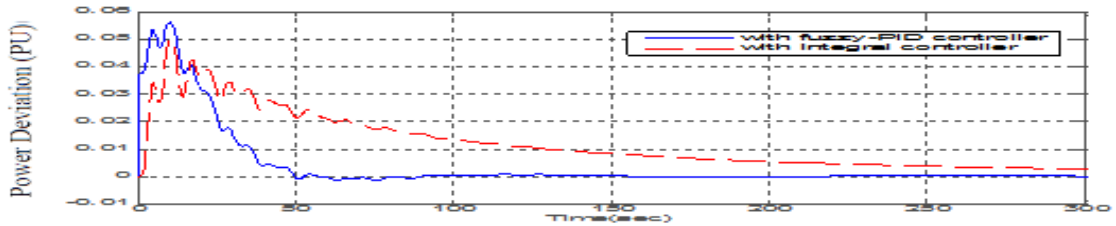


Figure (C 20) Generator output power of area -9- (ΔP_{g9})

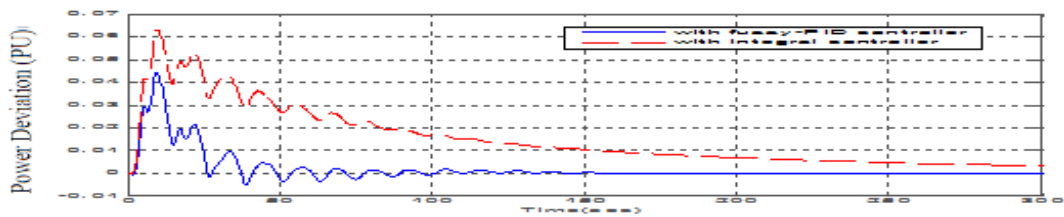


Figure (C 21) Generator output power of area -10 -(ΔP_{g10})

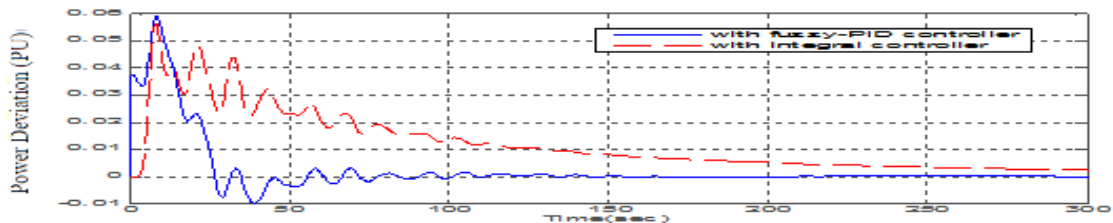


Figure (C 22) Generator output power of area -11-(ΔP_{g11})

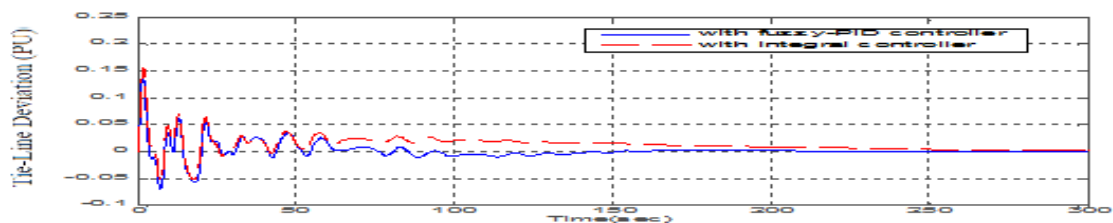


Figure (C 23) Tie-line power response ($\Delta p_{tie_{1,2}}$) –

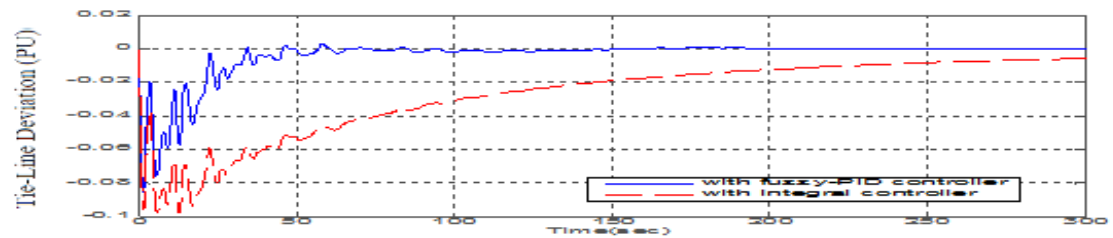


Figure (C 24) Tie-line power response ($\Delta p_{tie_{2,3}}$) –

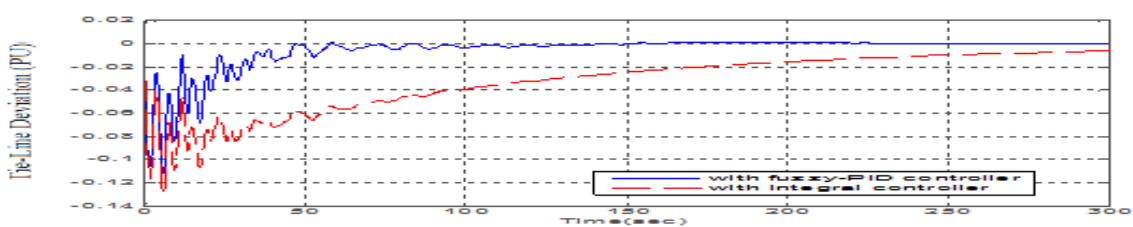


Figure (C 25) Tie-line power response ($\Delta p_{tie_{2,5}}$)

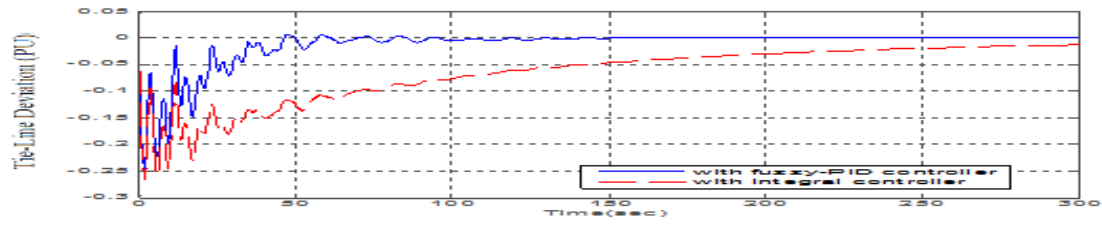


Figure (C 26) Tie-line power response ($\Delta ptie_{2,8}$)

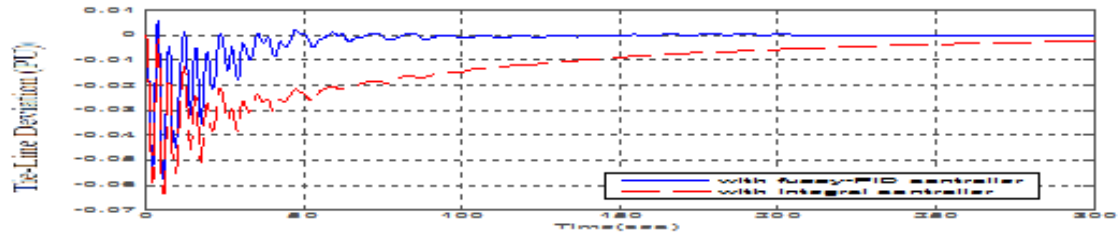


Figure (C 27) Tie-line power response ($\Delta ptie_{3,4}$)

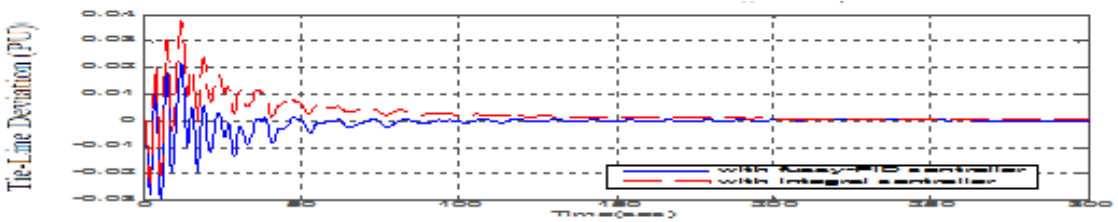


Figure (C 28) Tie-line power response ($\Delta ptie_{4,6}$) –

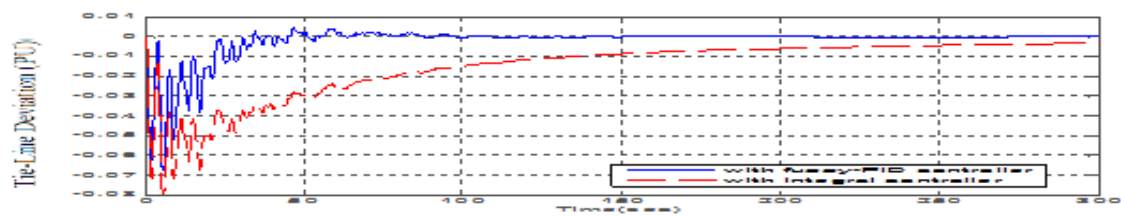


Figure (C 29) Tie-line power response ($\Delta ptie_{5,7}$)

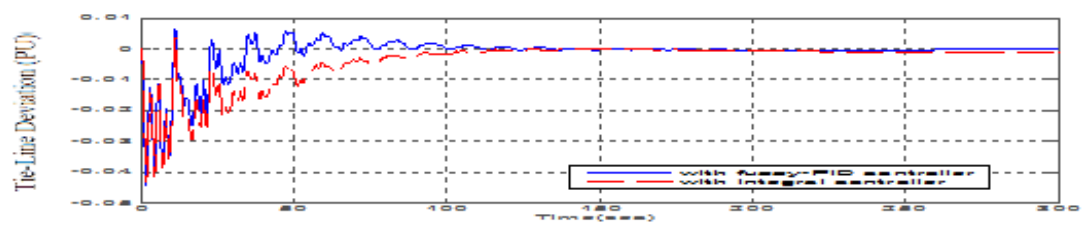


Figure (C 30) Tie-line power response ($\Delta ptie_{5,8}$)

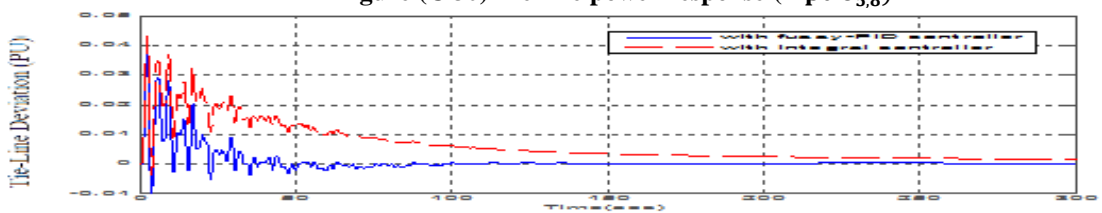


Figure (C 31) Tie-line power response ($\Delta ptie_{6,7}$)

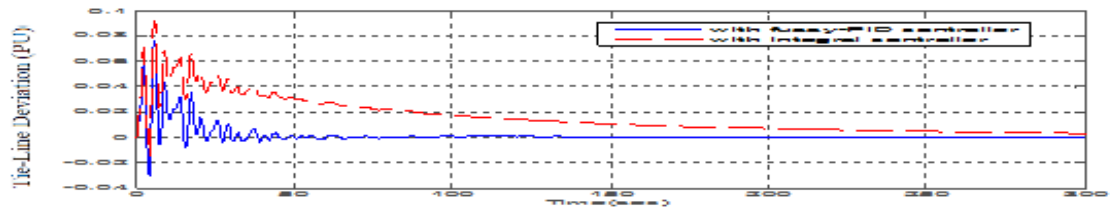


Figure (C 32) Tie-line power response ($\Delta tie_{6,8}$)

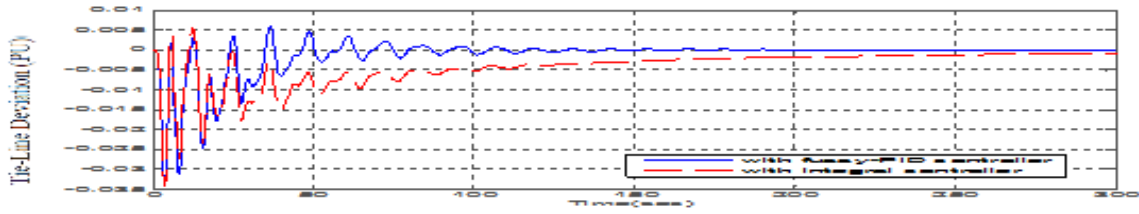


Figure (C 33) Tie-line power response ($\Delta tie_{6,9}$)

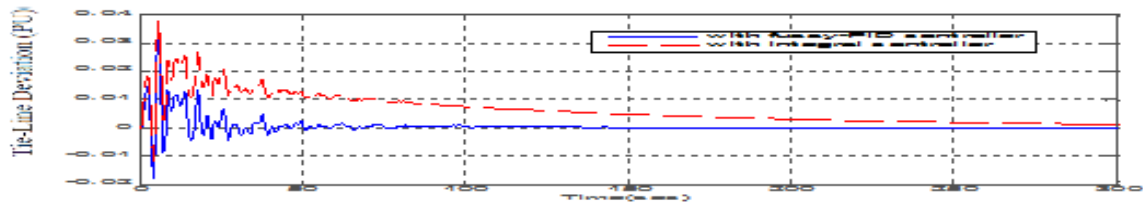


Figure (C 34) Tie-line power response ($\Delta tie_{7,8}$)

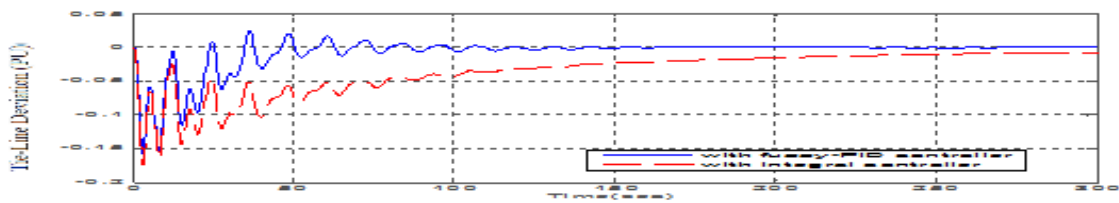


Figure (C 35) Tie-line power response ($\Delta tie_{8,9}$)

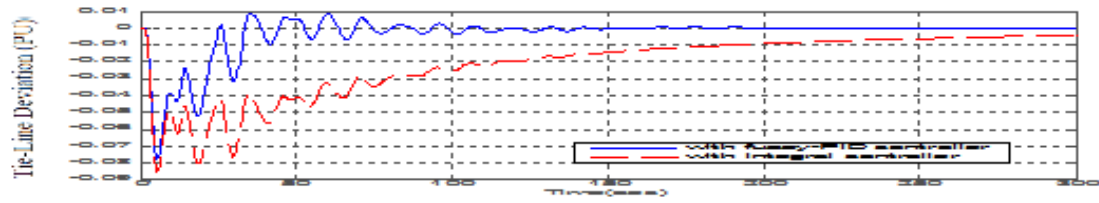


Figure (C 36) Tie-line power response ($\Delta tie_{9,10}$)

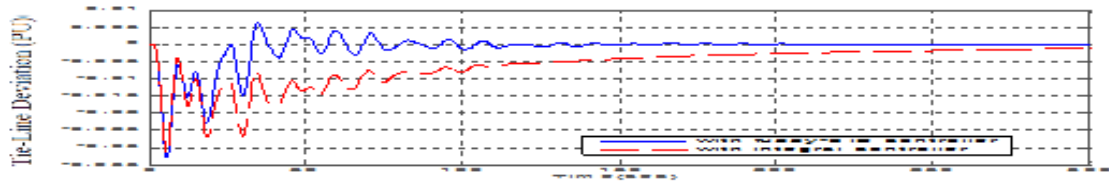


Figure (C 37) Tie-line power response ($\Delta tie_{9,11}$)

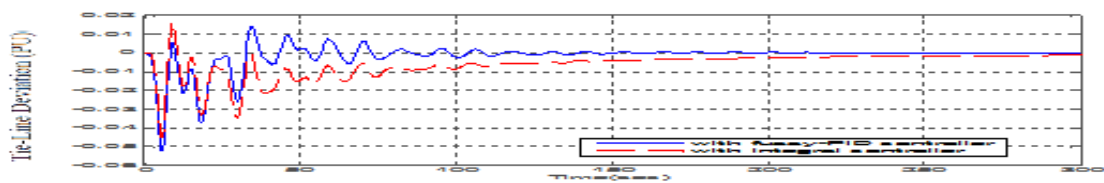


Figure (C 38) Tie-line power response ($\Delta tie_{10,11}$)

خوارزمية لمنظم التوليد الذاتي لشبكة القدرة الكهربائية العراقية باستخدام تقنية المنطق المضبيب

الخلاصة:

يقترح هذا العمل خوارزمية مبنية على تقنية المنطق الضبابي لوحدة تحكم نظام الطاقة (AGC) لتعزيز أداء وحدة التحكم التقليدية خلال الحالة الطبيعية وغير الطبيعية (الاختلاف في الحمل) للشبكة .
تم دراسة السلوك الديناميكي لمنظومة نقل الطاقة الفائقة العراقية (400 kV) في الحالة الطبيعية ومع تغير الحمل بمقدار 10% (كحالة خطرة) باستخدام المنظمين التقليدي والمقترح باستخدام برنامج MATLAB/SIMULINK .
اظهرت النتائج فعالية الطريقة المقترحة في تحسين الاداء الديناميكي للشبكة مقارنة بالمسيطرات التقليدية من حيث الدقة ومن حيث تقليل زمن استقرارية المنظومة (Overshoot and settling time)